Optics Communications 391 (2017) 1–8

Contents lists available at ScienceDirect

Optics Communications

journal homepage: www.elsevier.com/locate/optcom

Eliminating the influence of source spectrum of white light scanning interferometry through time-delay estimation algorithm

Yunfei Zhou[a], Hongzhi Cai[a], Liyun Zhong[a], Xiang Qiu[a], Jindong Tian[b], Xiaoxu Lu[a,*]

[a] Guangdong Provincial Key Laboratory of Nanophotonic Functional Materials and Devices, South China Normal University, Guangzhou 510006, China
[b] College of Optoelectronic Engineering, Shenzhen University, Shenzhen 518060, China

ARTICLE INFO

Keywords:
Profile measurement
White light scanning interferometry (WLSI)
Time-delay estimation
Interference signal envelope

ABSTRACT

In white light scanning interferometry (WLSI), the accuracy of profile measurement achieved with the conventional zero optical path difference (ZOPD) position locating method is closely related with the shape of interference signal envelope (ISE), which is mainly decided by the spectral distribution of illumination source. For a broadband light with Gaussian spectral distribution, the corresponding shape of ISE reveals a symmetric distribution, so the accurate ZOPD position can be achieved easily. However, if the spectral distribution of source is irregular, the shape of ISE will become asymmetric or complex multi-peak distribution, WLSI cannot work well through using ZOPD position locating method. Aiming at this problem, we propose time-delay estimation (TDE) based WLSI method, in which the surface profile information is achieved by using the relative displacement of interference signal between different pixels instead of the conventional ZOPD position locating method. Due to all spectral information of interference signal (envelope and phase) are utilized, in addition to revealing the advantage of high accuracy, the proposed method can achieve profile measurement with high accuracy in the case that the shape of ISE is irregular while ZOPD position locating method cannot work. That is to say, the proposed method can effectively eliminate the influence of source spectrum.

1. Introduction

With the development of specific manufacturing technology, MEMS device and semiconductor chip have been widely used, and the corresponding three-dimension (3D) profile measurement with high accuracy and rapid speed is becoming more and more needed [1]. Atomic force microscopy (AFM) possesses high resolution, but there are some limitations in the scanning speed and the measuring range for 3D profile measurement [2,3]. Though single-wavelength interferometry reveals the advantages of whole-field, high accuracy, non-contact and non-destruction [4], the phase-ambiguity problem make it is suitable for only smooth surface measurement due to its measuring range of height is less than $\lambda/2$ [5]. To address this, white light scanning interferometry (WLSI) is introduced through using zero optical path difference (ZOPD) position locating method, so the corresponding measuring range of height is enlarged [6]. To date, WLSI has been widely used in 3D profile measurement, automatic processing, product quality control and other fields [7].

As we know, WLSI utilizes a broadband light as the illumination source, if the optical path difference between the object beam and reference beam is smaller than the coherence length of illumination source, the interference signal will appear. Thus, the intensity distribution of a measured point of sample can be described as a cosine function modulated by an envelope [8]. If the optical path difference between the object beam and reference beam is equal to zero, the intensity maximum of interference signal, named as the zero optical path difference (ZOPD) position, can be observed [9]. Typically, by using a piezoelectric ceramic transducer (PZT) stage drives the measured object, the interference signal reflecting the ZOPD position can be achieved. Following, by searching for ZOPD position of each pixel, the profile of the measured object can be constructed. That is to say, ZOPD position locating is an important research content of WLSI. To date, many ZOPD position location methods of WLSI have been reported. In general, these methods are classified into two types. One type is to search for the peak position of interference signal envelope (ISE), such as the barycenter method [10], Fourier transform [11] and Hilbert transform [8]. The other one is to determine ZOPD position location through introducing the phase retrieval algorithm, such as spatial frequency domain analysis [9,12], continuous wavelet transform [13], windowed Fourier transform [14]

* Corresponding author.
E-mail address: hsgdzlxx@scnu.edu.cn (X. Lu).

http://dx.doi.org/10.1016/j.optcom.2016.12.006
Received 15 July 2016; Received in revised form 30 October 2016; Accepted 3 December 2016

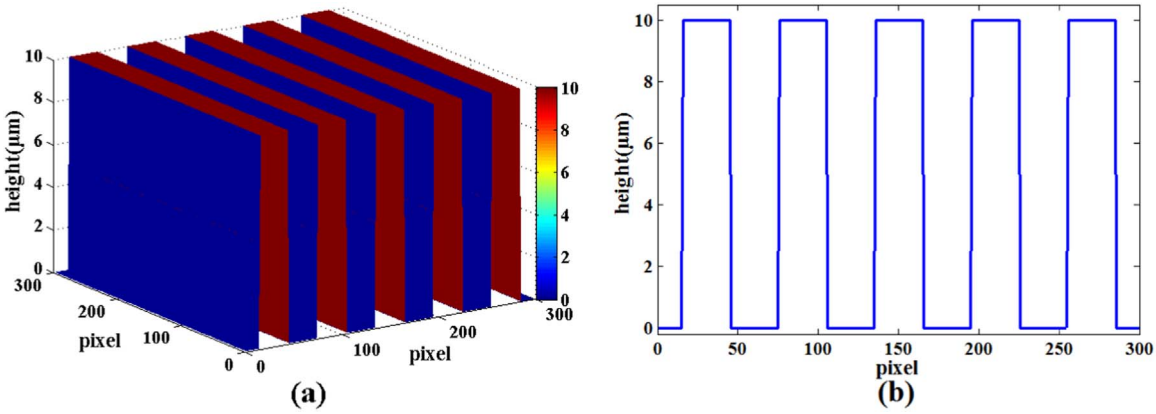

Fig. 1. (a) Profile of the simulated object; (b) the corresponding cross-section distribution of (a).

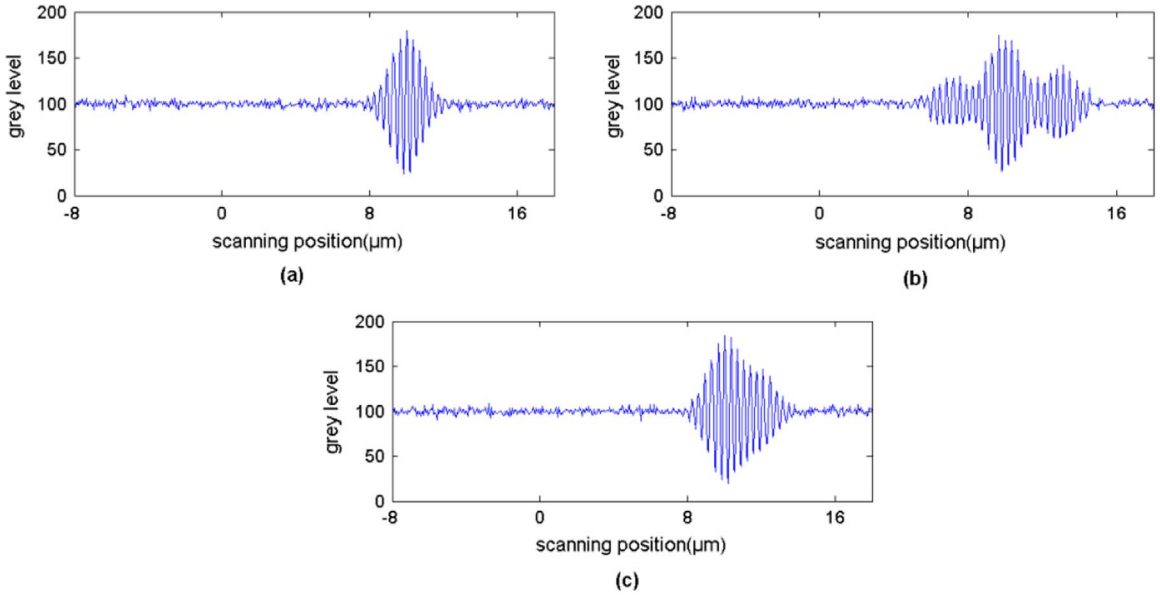

Fig. 2. The simulated intensity distribution of interference signal in pixel (100, 100) with different envelope functions, (a) symmetric distribution $g1$; (b) multi-peak distribution $g2$; (c) asymmetric distribution $g3$.

and white light phase-shifting method [15,16]. However, the above methods are suitable only for the ISE with symmetrical shape, if the shape of ISE is irregular, the error of ZOPD position locating will appear. Specially, various broadband sources with different spectral distribution are utilized in WLSI, so the shape of ISE will be different. Though several researches about the error of ZOPD position locating induced by broadband source have been reports [17,18], how to achieve accurate ZOPD position locating for different broadband sources is still required.

In this study, we introduce time-delay estimation (TDE) method [19,20] into WLSI, in which the broadband source is thought as a signal generator, and interference signals come from different object points are handled as the homologous time-delay signals. Thus the profile of the measured object can be calculated through calculating the time-delay of the interference signal of each pixel, reflecting the relative displacement of ZOPD position of each pixel. Next, we will present the principle, and then give the simulation and experimental result to verify the feasibility of ISE shape through using the proposed method.

2. Principle

According to the principle of TDE, two homologous signals with noise captured by two receivers can be respectively expressed as [20]

$$\begin{aligned} x_1(t) &= \alpha f(t) + n_1(t) \\ x_2(t) &= \beta f(t+D) + n_2(t) \end{aligned} \tag{1}$$

where $f(t)$ denotes the practical intensity of signal; $n_1(t)$ and $n_2(t)$ denote the noise; D is the time-delay between $x_1(t)$ and $x_2(t)$; there is no the correlation relationship between $f(t)$ and $n_1(t)$ or $n_2(t)$. Following, we utilize the cross-correlation method to calculate the time-delay D through using the cross-correlation function $R_{x_1x_2}(\tau)$

$$R_{x_1x_2}(\tau) = \int_0^\infty x_1(t)x_2(t-\tau)dt \tag{2}$$

Clearly, when $R_{x_1x_2}(\tau)$ reaches the maximum, τ is equal to the time-delay D. In the practical situation, the cross-correlation method usually leads to the calculating error of D due to the influence of noise. To address this, the generalized cross-correlation method is employed to remove the noise through the filter processing. If $I_1(f)$ and $I_2(f)$ are respectively the Fourier transform spectra of $x_1(t)$ and $x_2(t)$, the corresponding cross-power spectrum can be expressed as

$$G_{x_1x_2}(f) = I_1(f)[I_2(f)]^* \tag{3}$$

where * represents the complex conjugate operation. Then, $R_{x_1x_2}(\tau)$ can be expressed as

$$R_{x_1x_2}(\tau) = \int_{-\infty}^{\infty} G_{x_1x_2}(f)\exp(j2\pi f\tau)d\tau \tag{4}$$

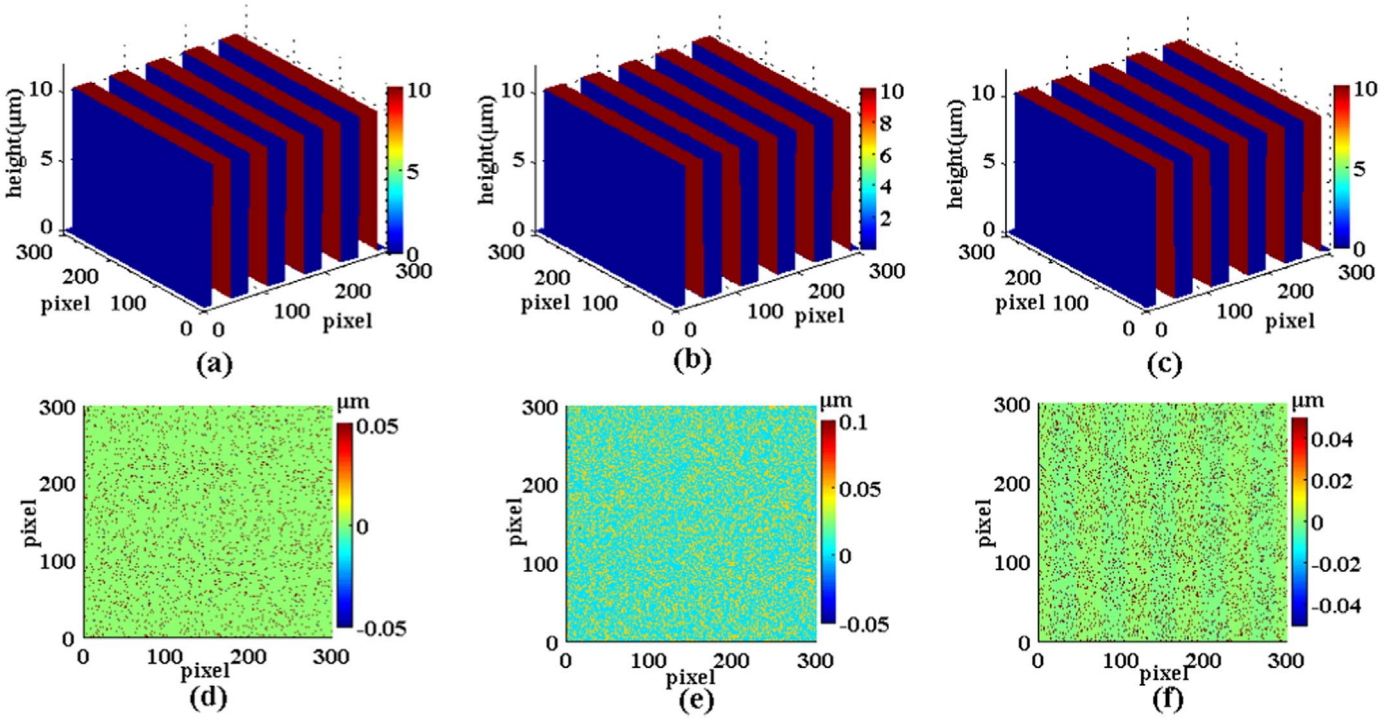

Fig. 3. The profile of the simulated object and the difference between preset value and the obtained height from the interference signal with different envelope functions of (a), (d) $g1$; (b), (e) $g2$; (c), (f) $g3$.

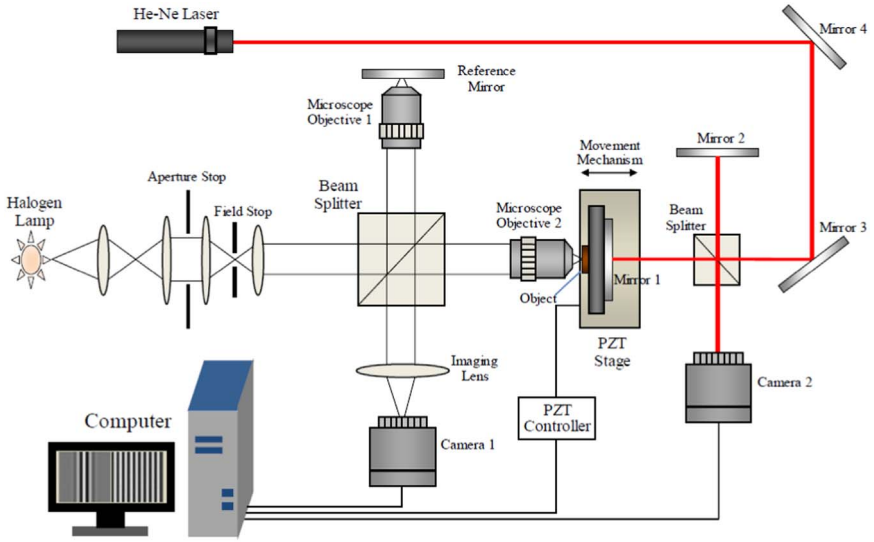

Fig. 4. Schematic of WLSI experimental system.

After the filter processing for $I_1(f)$ and $I_2(f)$, the cross-power spectrum can be rewritten as

$$G(f) = H_1(f)[H_2(f)]^* I_1(f)[I_2(f)]^* \tag{5}$$

where $H_1(f)$ and $H_2(f)$ denote filtering window.

And the generalized cross-correlation function between $x_1(t)$ and $x_2(t)$ can be written as

$$R(\tau) = \int_{-\infty}^{+\infty} G(f)\exp(j2\pi f\tau)dt \tag{6}$$

If Eq. (6) reaches the maximum, we can achieve the time-delay D. In WLSI, the intensity distribution of interference pattern captured a camera can be described as

$$I(x, y, z) = a(x, y) + b(x, y)g[z - h(x, y)]\cos\{\frac{4\pi}{\lambda_0}[z - h(x, y)]\} + n \tag{7}$$

where (x, y) represents the pixel coordinate of interference pattern, z is the vertical scanning coordinate along the optical axis; $h(x, y)$ denotes the height of measured object, $a(x, y)$ and $b(x, y)$ represent the background intensity and the modulation amplitude of interference pattern, respectively; $g[z\text{-}h(x, y)]$ denotes the interference signal envelop (ISE), λ_0 and n are the center wavelength of white light source and the random noise in the interference pattern.

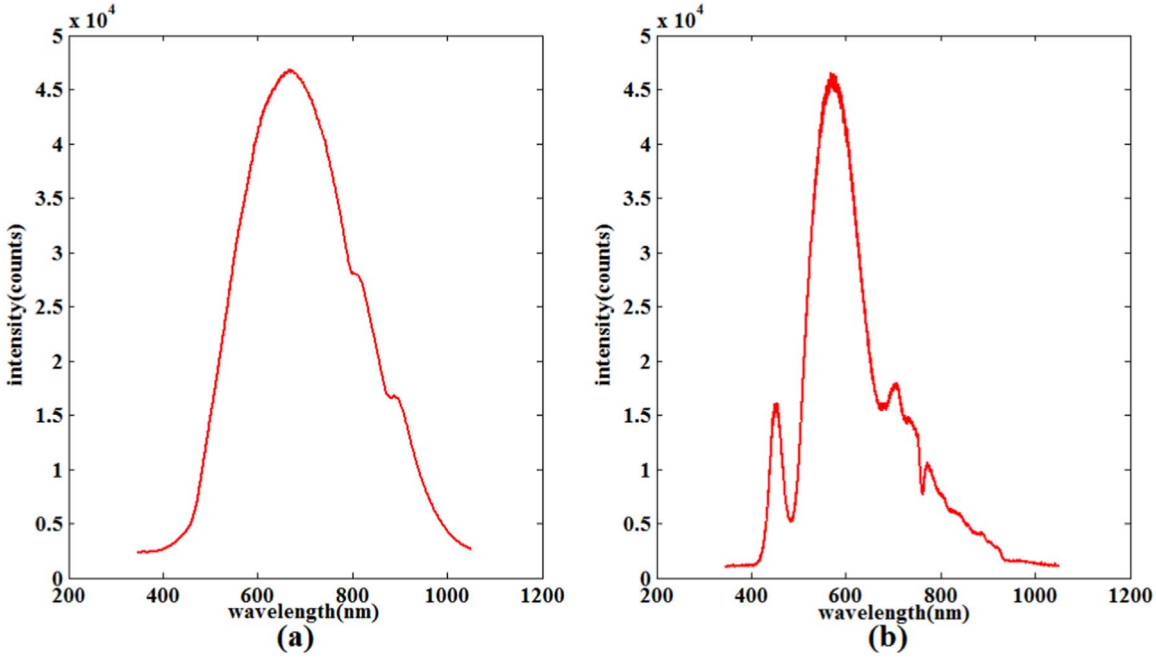

Fig. 5. Spectral distributions of (a) halogen lamp; (b) white light LED.

In WLSI, if a broadband source has only one peak that is in Gaussian distribution in its spectrum, the shape of ISE will reveal a symmetric distribution, the accurate ZOPD position of each pixel can be calculated from Eq. (7) easily. However, if a broadband source with non-Gaussian spectral distribution is utilized, the shape of ISE will show an asymmetric or complex multi-peak distribution; this will lead a large error of ZOPD position locating. To address this, we introduce the TDE method into WLSI, in which the broadband source is regarded as a signal generator, the interference signals of different points are thought as the homologous signals with noise captured by different receivers. Thus, the ZOPD position locating of measured pixel can be replaced by calculating the time-delay of interference signal between the measured pixel and a selected pixel. Next, we will give the calculating process.

From Eq. (7), the intensity signal of pixel (x_1, y_1) and (x_2, y_2) can be respectively expressed as

$$\begin{aligned} I(x_1, y_1, z) &= a(x_1, y_1) + b(x_1, y_1) g[z - h(x_1, y_1)] \cos\{\tfrac{4\pi}{\lambda_0}[z - h(x_1, y_1)]\} \\ &\quad + n_1 \\ I(x_2, y_2, z) &= a(x_2, y_2) + b(x_2, y_2) g[z - h(x_2, y_2)] \cos\{\tfrac{4\pi}{\lambda_0}[z - h(x_2, y_2)]\} \\ &\quad + n_2 \end{aligned} \tag{8}$$

By using the generalized cross-correlation method, we can achieve $\Delta h = h(x_2, y_2) - h(x_1, y_1)$ through $I(x_1, y_1, z)$ and $I(x_2, y_2, z)$ corresponding to $x_1(t)$ and $x_2(t)$ of Eq. (1), respectively.

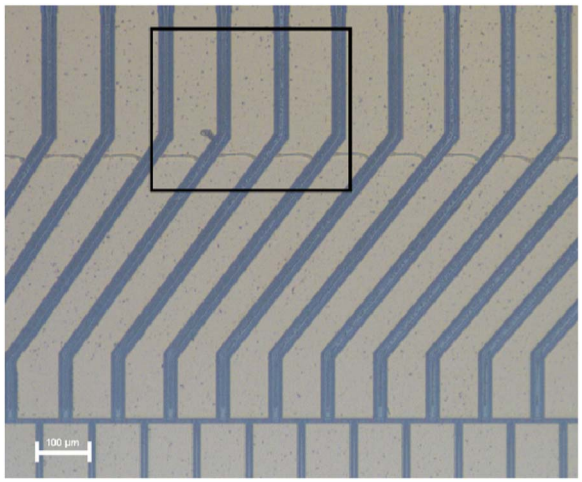

Fig. 6. Microimage of an optical switch MEMS device, in which the black rectangular denotes the measured area.

3. Numerical simulation

The numerical simulation is employed to verify the validity of the proposed method. First, we use a reflective object, containing five steps with height of 10 μm and the same distance between adjacent steps, as the measured object. The size of interference pattern is 300×300 pixels (−1.5mm1≤x, y≤1.5 mm). The surface profile of simulated object and the corresponding cross-section distribution are presented in Fig. 1(a) and (b).

The intensity distribution of interference pattern is determined according to Eq. (7), in which the background intensity, modulation amplitude and center wavelength of white light source are set as a=100, b=80, λ_0=0.7 μm, the coherence length is equal to $l_c = \lambda_0^2/\Delta\lambda$, the spectral bandwidth is $\Delta\lambda$=0.4 μm, the random noise with 3% of background intensity is added to the interference pattern. The scanning interval is set as 0.05 μm and scanning range is equal to −8 μm to 18 μm. As shown in Fig. 2, we choose three interference signals with different ISE to calculate the surface profile of measured object. Three envelope functions are set as $g1[z - h(x, y)] = \exp\{-[z - h(x, y)]^2/l_c^2\}$, $g2[z - h(x, y)]$-
$=\exp\{-[z - h(x, y)]^2/l_c^2\} + \exp\{-[z - h(x, y) - 3]^2/l_c^2\}/2$,-
$+ \exp\{-[z - h(x, y) + 3]^2/l_c^2\}/3$
$g3[z - h(x, y)] = \exp\{-[z - h(x, y)]^2/l_c^2\} + \exp\{-[z - h(x, y) - 2]^2/l_c^2\}$,
/2
as shown in Fig. 2(a–c), respectively.

Using the proposed TDE method, we calculate the surface profiles

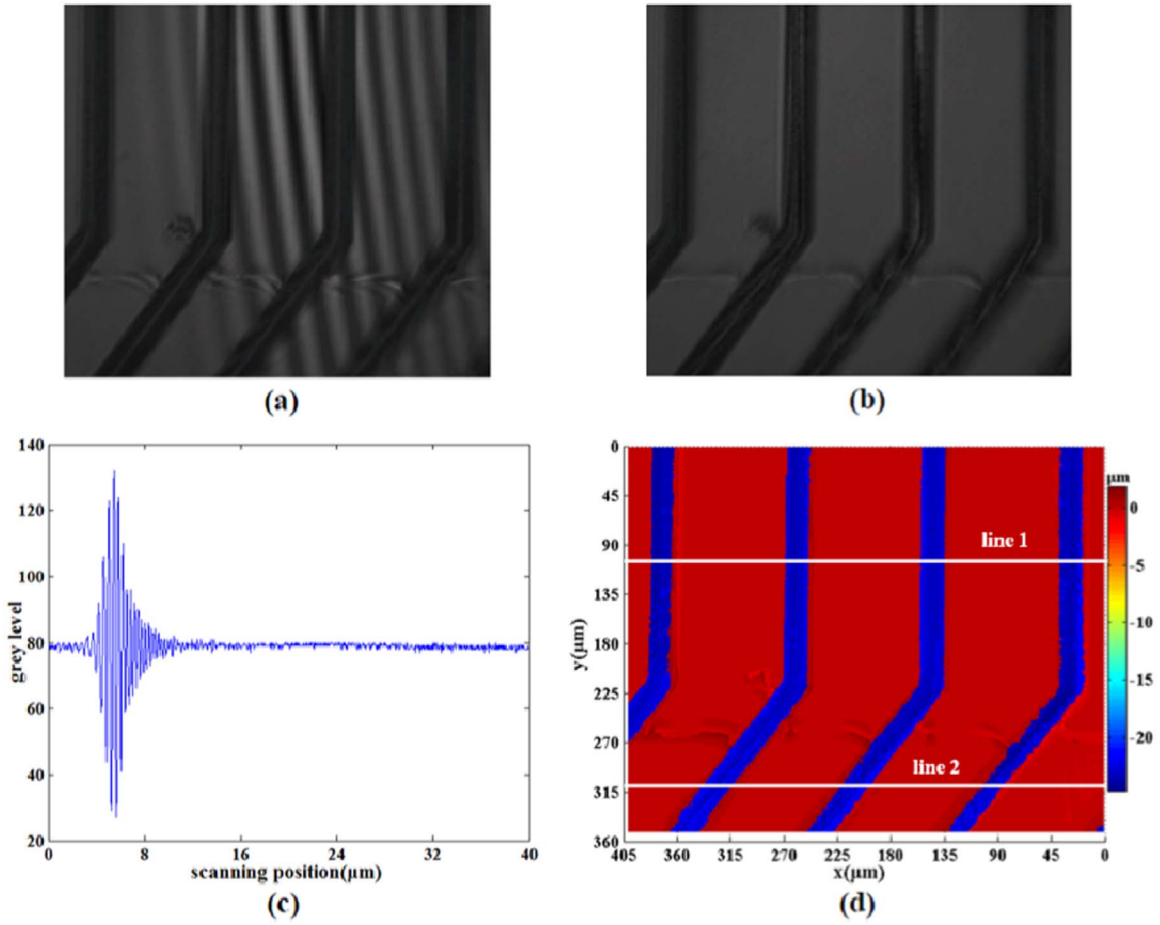

Fig. 7. Using the halogen lamp as light source, (a), (b) two interference patterns of MEMS device captured in two PZT scanning positions; (c)the intensity distribution of one pixel of interference pattern; (d) the surface profile of MEMS device achieved with the proposed method.

of the measured object from above three interference signals, as shown in Fig. 3(a–c), respectively; and Fig. 3(d–f) show the differences between the preset value and the obtained height, respectively. It is found that the root mean square error (RMSE) of the difference between the preset value and the obtained height are respectively 12.7 nm, 23.7 nm and 15.8 nm, indicating that the proposed method can be utilized in different type ISEs.

4. Experimental results and discussion

Next, we utilize a WLSI experimental system to present the feasibility of the proposed method, as shown in Fig. 4. After passing through Kohler illumination system, a broadband light is split into the object beam and reference beam by splitting prism 1; the reference beam goes through micro-objective 1 and reflected by a reference mirror, and object beam goes through micro-objective 2 and reflected by the measured object, in which the magnification of micro-objective 1 and micro-objective 2 is same. The object beam and reference beam superpose and interference on splitting prism 1 and received by digital camera 1 through an imaging lens. And a piezoelectric ceramic transducer (PZT) stage is employed to drive the vertical scanning of measured object, if the ZOPD position between object beam and reference beam appears, the interference fringe can be observed. Usually, to achieve the accurate ZOPD position, it is required to calibrate the displacement of PZT device in advance. In this study, we introduce a laser Michelson interferometry system to calibrate the vertical scanning displacement of PZT stage, in which a standard flat mirror 1 is fixed on the measured object platform, so the movement of measured object is same with mirror 1. Through using the laser interference pattern captured by digital camera 2, we can calculate the scanning displacement of mirror 1 and achieve the displacement calibration of PZT stage [21]. Following, using this WLSI experimental system, if PZT device moves a step-interval, camera 1 and camera 2 can simultaneously capture the white light interference pattern and laser interference pattern, respectively. Thus, the calibration of PZT scanning and surface profile measurement can be achieved simultaneously.

Next, we respectively utilize a halogen lamp and a white light LED as source to measure the surface profile of an optical switch MEMS device. Fig. 5(a) and (b) respectively show the spectral distribution of halogen lamp and white light LED captured by a spectrometer (Ocean Optics, USB4000). We can see that the halogen lamp reveals Gaussian distribution in its spectrum with only one peak while the white light LED shows non-Gaussian distribution with multi-peak in its spectrum. Fig. 6 gives the microimage of measured optical switch MEMS device captured by a microscope (Nikon, Ti), in which the black rectangular denotes the measured area. A PZT displacement stage (NewPi, XP-612.XY80S and XE-501 controller) is utilized to achieve the vertical scanning. Camera 1 and 2 are two digital CMOS camera (DH-HV1303UM); the magnifications of micro-objective 1 and micro-objective 2 are equal to 10×, and the step-interval of PZT moving is set as 40 nm.

Although the signals would be different at different points, they have the same shape of ISE corresponding to the spectral distribution of light source. It does not affect finding the maximum value of cross-correlation function or calculating the time-delay D. In addition, there should be no film-like covering on the MEMS device's surface to avoid multiple-reflection and overlapped envelope.

Using the halogen lamp as illumination source, Fig. 7(a) and (b)

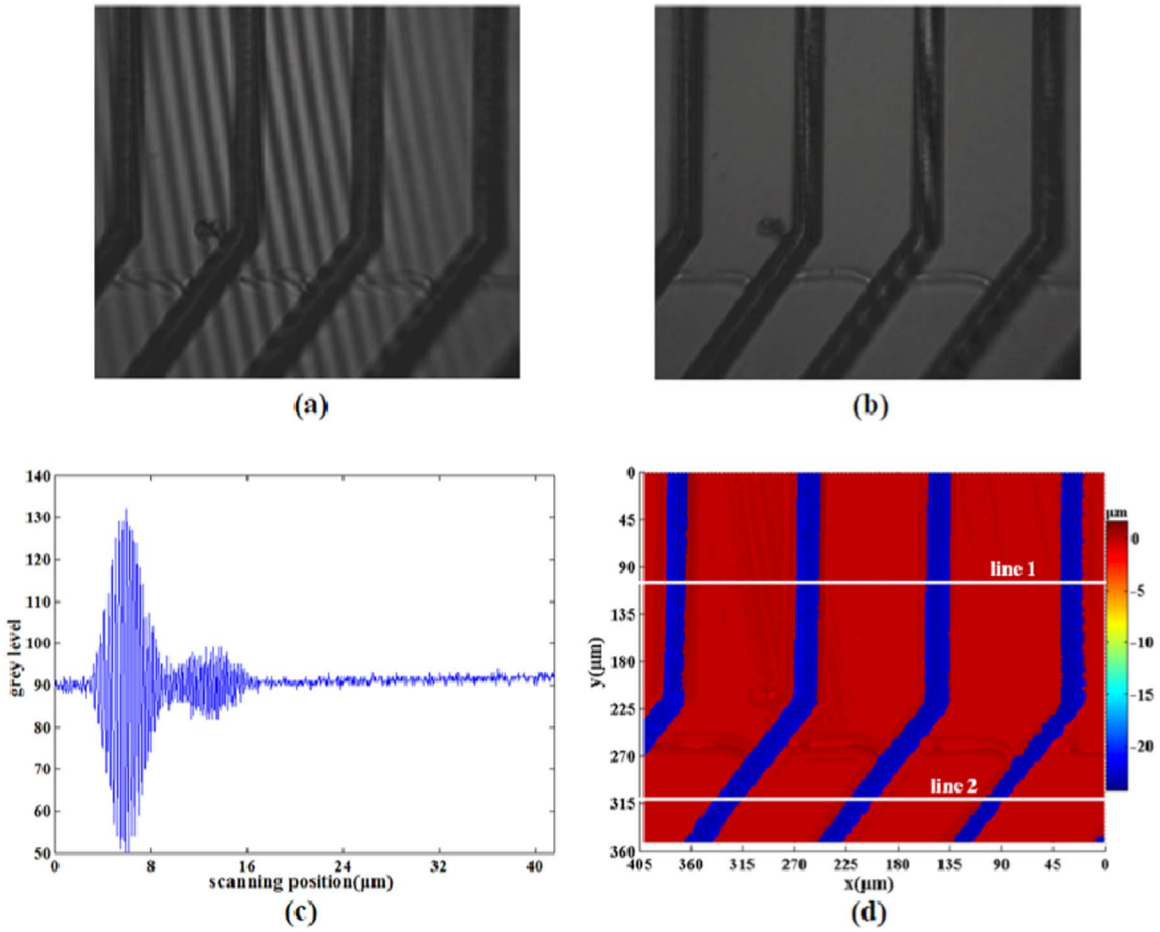

Fig. 8. Using a white light LED as source, (a), (b) two interference patterns of MEMS device captured in two different PZT scanning positions; (c) the intensity distribution of one pixel of interference pattern; (d) the surface profile of MEMS device achieved with the proposed method.

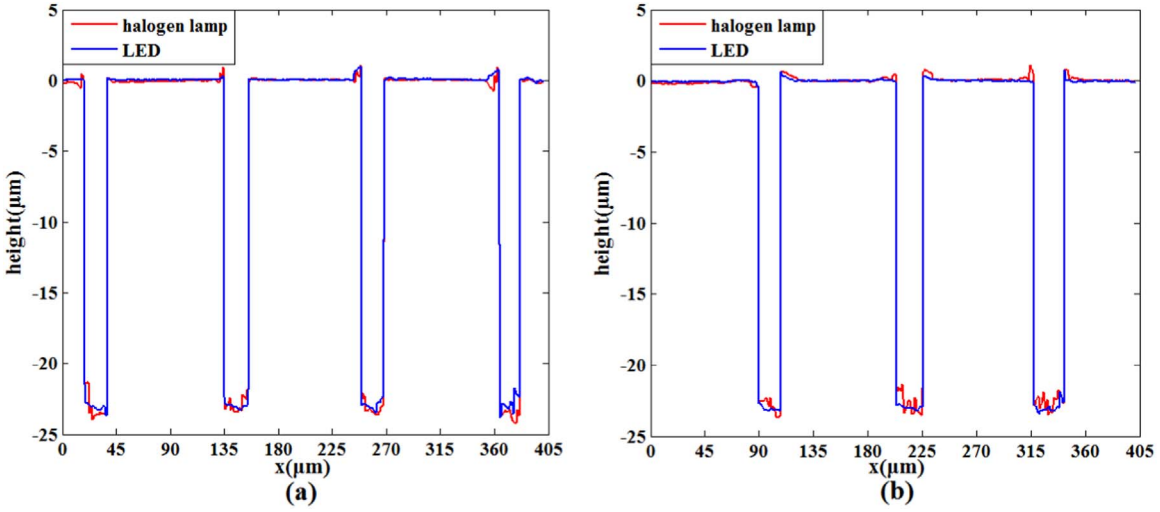

Fig. 9. Cross-section distributions of (a) white line 1; (b) white line 2 in Fig. 7(d) and Fig. 8(d), respectively.

present two interference patterns of measured MEMS device captured in two PZT scanning positions; Fig. 7(c) gives the intensity distribution of one pixel of interference pattern, and Fig. 7(d) shows the corresponding surface profile achieved with the proposed method.

Similarly, using the white light LED as illumination source, Fig. 8(a–d) give the corresponding experimental results. In addition, to compare the measuring accuracy through using halogen lamp and LED as source, Fig. 9(a) and (b) show the cross-section distributions of white line 1 and white line 2 in Fig. 7(d) and Fig. 8(d), respectively. In contrast, we also give the surface profile of MEMS device achieved with ZOPD position locating method (Fourier transform), as shown in Fig. 10. It is found that using the proposed method, the accuracy of

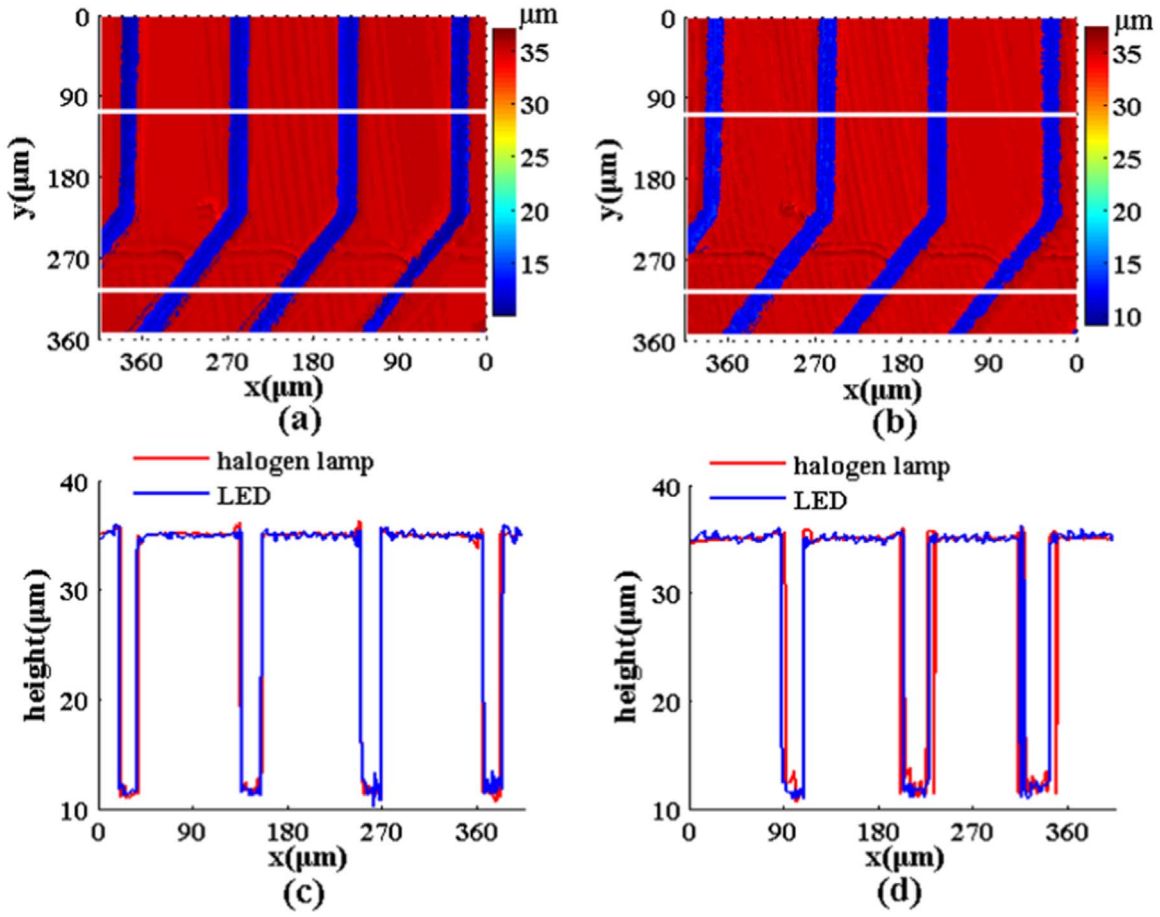

Fig. 10. Surface profiles of MEMS device achieved with ZOPD position locating method through using different sources (a) halogen lamp; (b) white light LED; (c) and (d) the cross-section distributions of white line 1 and white line 2 in (a) and (b), respectively.

profile measurement with the halogen lamp is nearly the same with the white light LED while ZOPD position locating method cannot work well. From these results, we can find that the proposed method can achieve high accuracy surface profile whether using the halogen lamp or white light LED as source in WLSI. That is to say, using the proposed method, the influence of source spectrum of WLSI can be effectively eliminated.

5. Conclusion

In WLSI, the accuracy of ZOPD position locating is closely related with the shape of ISE, which is mainly decided by the spectral distribution of illumination source. For a broadband light with Gaussian spectral distribution, the corresponding shape of ISE reveals a symmetric distribution, and it is easy to achieve high accuracy profile measurement through using ZOPD position locating method. However, if the spectral distribution of illumination source is irregular, the corresponding shape of ISE may be the asymmetric or complex multi-peak distribution, and this will lead to a large error of ZOPD position locating. In this study, we introduce a new TDE method into WLSI, in which the surface profile information is achieved with the relative displacement of interference signal between different pixels instead of the conventional ZOPD position locating method. Due to all spectral information of interference signal (envelope and phase) are utilized, the proposed method can improve the accuracy of surface profile measurement. Specially, in the case that the shape of ISE is irregular, the proposed method can achieve profile measurement with high accuracy while the conventional ZOPD position locating method cannot work. Both the simulation and the experimental results demonstrate that in addition to revealing the advantage of high accuracy, the proposed method can effectively eliminated the influence of source spectrum of WLSI. This will greatly facilitate the application of TDE based WLSI.

Acknowledgment

This work is supported by National Nature Science Foundation of China grants (61177005, 61275015 and 61475048).

References

[1] C. O'Mahony, M. Hill, M. Brunet, R. Duane, A. Mathewson, Characterization of micromechanical structures using white-light interferometry, Meas. Sci. Technol. 14 (2003) 1807–1814.
[2] N.H. Green, S. Allen, M.C. Davies, C.J. Roberts, S.J.B. Tendler, P.M. Williams, Force sensing and mapping by atomic force microscopy, trac-trend, Anal. Chem. 21 (2002) 64–73.
[3] A. Peled, J. Castro, J. Weiss, Atomic force microscopy examinations of mortar made by using water-filled lightweight aggregate, Transp. Res. Rec. 2141 (2010) 92–101.
[4] Z. Wangping, L. Xiaoxu, L. Chunshu, Z. Liyun, J. Vargas, Principal component analysis based simultaneous dual-wavelength phase-shifting interferometry, Opt. Commun. 341 (2015) 276–283.
[5] F. Salzenstein, P. Montgomery, A. Boudraa, Local frequency and envelope estimation by Teager-Kaiser energy operators in white-light scanning interferometry, Opt. Express 22 (2014) 18325–18334.
[6] G.S. Kino, S.S. Chim, Mirau correlation microscope, Appl. Opt. 29 (1990) 3775–3783.
[7] R. Windecker, H.J. Tiziani, Optical roughness measurements using extended white-light interferometry, Opt. Eng. 38 (1999) 1081–1087.
[8] S.S. Chim, G.S. Kino, Three-dimensional image realization in interference microscopy, Appl. Opt. 31 (1992) 2550–2553.
[9] P. de Groot, L. Deck, Surface profiling by analysis of white-light interferograms in the spatial frequency domain, J. Mod. Opt. 42 (1995) 389–401.

[10] S. Chen, A. Palmer, K. Grattan, B. Meggitt, Digital signal-processing techniques for electronically scanned optical-fiber white-light interferometry, Appl. Opt. 31 (1992) 6003–6010.
[11] S.S. Chim, G.S. Kino, Correlation microscope, Opt. Lett. 15 (1990) 579–581.
[12] P. de Groot, X.C. de Lega, J. Kramer, M. Turzhitsky, Determination of fringe order in white-light interference microscopy, Appl. Opt. 41 (2002) 4571–4578.
[13] P. Sandoz, Wavelet transform as a processing tool in white-light interferometry, Opt. Lett. 22 (1997) 1065–1067.
[14] S. Ma, C. Quan, R. Zhu, C. Tay, L. Chen, Z. Gao, Micro-profile measurement based on windowed Fourier transform in white-light scanning interferometry, Opt. Commun. 284 (2011) 2488–2493.
[15] K.G. Larkin, Efficient nonlinear algorithm for envelope detection in white light interferometry, J. Opt. Soc. Am. A 13 (1996) 832–843.
[16] J.T. Dong, R.S. Lu, A five-point stencil based algorithm used for phase shifting low-coherence interference microscopy, Opt. Lasers Eng. 50 (2012) 502–511.
[17] C.W. Keat, L. Xiang, S. Wijesoma, Effects of phosphor-based LEDs on vertical scanning interferometry, Opt. Lett. 35 (2010) 2946–2948.
[18] C.W. Keat, L. Xiang, S.Y. Chai, Harnessing spectral property of dual wavelength white LED to improve vertical scanning interferometry, Appl. Opt. 52 (2013) 4652–4662.
[19] C.H. Knapp, G.C. Carter, The generalized correlation method for estimation of time delay, IEEE Trans. Acoust. Speech Signal Process (1976) 320–327 ASSP-24.
[20] M. Azaria, D. Hertz, Time delay estimation by generalized cross correlation methods, IEEE Trans. Acoust. Speech Signal Process (1984) 280–285 ASSP-32.
[21] C. Luo, L. Zhong, P. Sun, H. Wang, J. Tian, X. Lu, Two-step demodulation algorithm based on the orthogonality of diamond diagonal vectors, Appl. Phys. B-Lasers O 119 (2015) 387–391.